Title: **Surface curvature-quantized energy and forcefield in geometrochemical physics**

Z. R. Tian, Chemistry/Biochemistry, and Materials Science/Engineering, University of Arkansas, Fayetteville, AR 72701, USA, (Email) rtian@uark.edu.

Most recently, simple-shape particles' surface area-to-volume ratio has been quantized into a geometro-wavenumber (ν_{Geo}), or geometro-energy (E_{Geo}) ≡ hc·ν_{Geo}, to quantitatively predict and compare nanoparticles (NPs), ions, and atoms geometry-quantized properties[1,2]. These properties range widely, from atoms' electronegativity (EN) and ionization potentials to NPs' bonding energy, atomistic nature, chemical potential of formation, redox potential, surface adsorbates' stability, and surface defects' reactivity. For countless irregular- or complex-shaped molecules, clusters, and NPs whose ν_{Geo} values are uneasy to calculate, however, the E_{Geo} application seems limited. This work has introduced smaller surfaces' higher curvature-quantized energy and forcefield for linking quantum mechanics, thermodynamics, electromagnetics, and Newton's mechanics with Einstein's general relativity. This helps quantize the gravity, gravity-counterbalancing levity, and Einstein's spacetime, geometrize Heisenberg's Uncertainty, and support many known theories consistently for unifying naturally the energies and forcefields in physics, chemistry, and biology.

Firstly, let's quantize shaper corners' and edges' greater surface curvature (1/r) into a spacetime wavenumber (ν_{ST}), i.e. Spacetime Energy (E_{ST}) = $hc(\nu_{ST})$ = *hc(1/r)* (see the **Fig. 3** below), where the r = particle radius, *h* = Planck constant, *c* = speed of light, and *hc* ≈ 1.24 (keV·nm). Indeed, smaller atoms' higher EN and smaller 0-dimensional (0D) NPs'

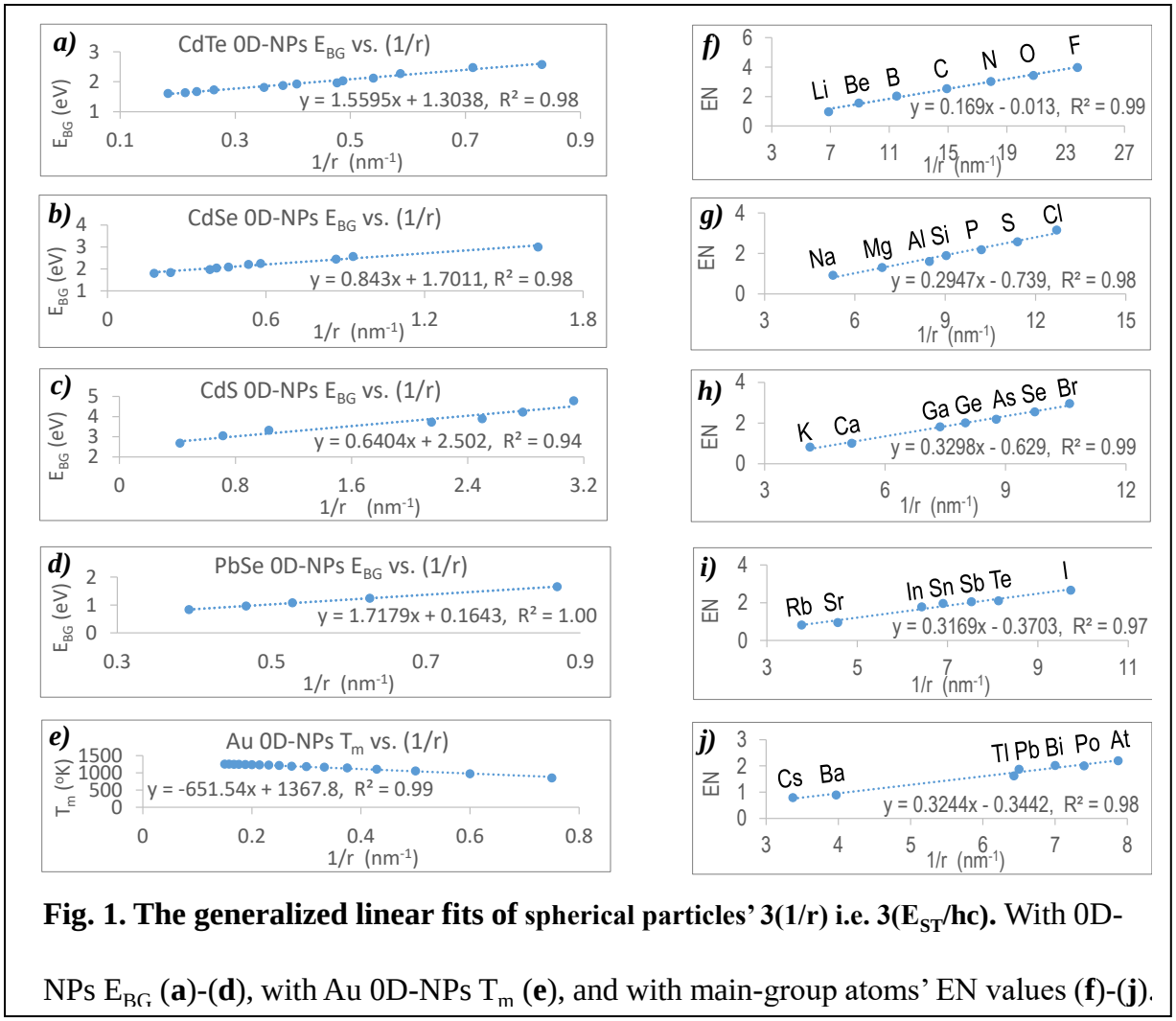

Fig. 1. The generalized linear fits of spherical particles' 3(1/r) i.e. 3(E_{ST}/hc). With 0D-NPs E_{BG} (**a**)-(**d**), with Au 0D-NPs T_m (**e**), and with main-group atoms' EN values (**f**)-(**j**).

lower melting point (T_m) and higher (i.e. more blue-shifted) optical bandgap (E_{BG}) (see the **Supplementary Table S1)**[3-9] are linearly governed by their greater (1/r) i.e. (E_{ST}/*hc*) (**Fig. 1**). Since a spherical particle's ν_{Geo} = $4\pi\cdot r^2/(4\pi\cdot r^3/3)$ = 3(1/r), i.e. $E_{Geo} \equiv hc\cdot\nu_{Geo}$ = $hc\cdot 3(1/r)$, or $E_{ST} = E_{Geo}/3$, the non-spherical structure's E_{Geo} simply averages all surface-curvatures' E_{ST}. The E_{ST}, proving the Surface Curvature–Energy Equivalence (SCEE), supports minute facet-, edge- and corner-surfaces' dangling bonds, and the E_{ST}-based chemical physics below.

For a nucleon ($r \approx 0.4 \times 10^{-6}$ nm)[10], for instance, its $E_{ST} = 1.24/(0.4 \times 10^{-6}) = 3.1$ (GeV), contrasting the $E_{(Nuclear\ Binding)} \leq 10$ (MeV)[11] (see the **Supplementary Information**). In a spherical particle's total

energy, the $E_{(surface)}$ (= E_{ST} = hc/r) unites the $E_{(potential)}$ (= m_oc^2, i.e. Einstein's mass-energy[12]) with the $E_{(kinetic)}$ (= pc, i.e. de Broglie's matter-wave[13] energy i.e. QM), where the m_o = particle rest mass, and p = particle momentum.

By the energy–force relation, the Spacetime Force (F_{ST}) = E_{ST}/d (see the **Fig. 3**), where the d = distance to the curving surface. Thus, the convex surfaces' positive curvature-quantized repulsing $F_{ST(convex)} > 0$ (like a positive charge's outward forcefield), and concave surfaces' negative curvature-based attractive $F_{ST(concave)} < 0$ (like a negative charge's inward forcefield). The repulsing $F_{ST(convex)}$ couples with the attracting $F_{ST(concave)}$ (like that between opposite point-charges, see the **Supplementary Fig. S1**), pushing a freestanding smaller S-shaped string (**Fig. 2a**) (or spiral, e.g. DNA- and/or α-helices) to rotate faster.

Given a nanoshell's inner concave surface's negative (–1/r)-based attracting force $\vec{F}_{ST(A)} = –hc/(rd)$, thickness *y*, and outer convex surface's positive {1/(r + *y*)}-based repulsing force $\vec{F}_{ST(R)} = hc/\{d(r + y)\}$, the $\vec{F}_{ST(nanoshell)} = (\vec{F}_{ST(R)} + \vec{F}_{ST(A)}) = –hcy/(r^2d + ryd)$. Symmetrically, the $\vec{F}_{ST(nanoshell)}$ should couple with the atom's $\vec{F}_{ST(R)}$ and Earth's $\vec{F}_{ST(A)}$ (**Fig. 2b**).

Between close-packed smaller particles, the smaller void's greater ($\vec{F}_{ST(shell)}$-like) $\vec{F}_{ST(A)}$ should pull the particles closer. This can help quantify self-assemblies' $\vec{F}_{ST(A)}$-based bonding to expand the Chemical Bonding Theory[3], and attribute a planet's mass-induced gravity to the voids (or vacuums) of all sizes, i.e. $\vec{F}_{(gravity)} = \Sigma\vec{F}_{ST(void)}$ (**Supplementary Information**).

Accordingly, a particle can migrate steadily (or stay still) when the surrounding net $\vec{F}_{ST(Net)} = 0$, acceleratively when the $\vec{F}_{ST(Net)} > 0$, deceleratively when the $\vec{F}_{ST(Net)} < 0$, and rotate when passing by another particle (**Fig. 2c**). This supports the F_{ST}-based

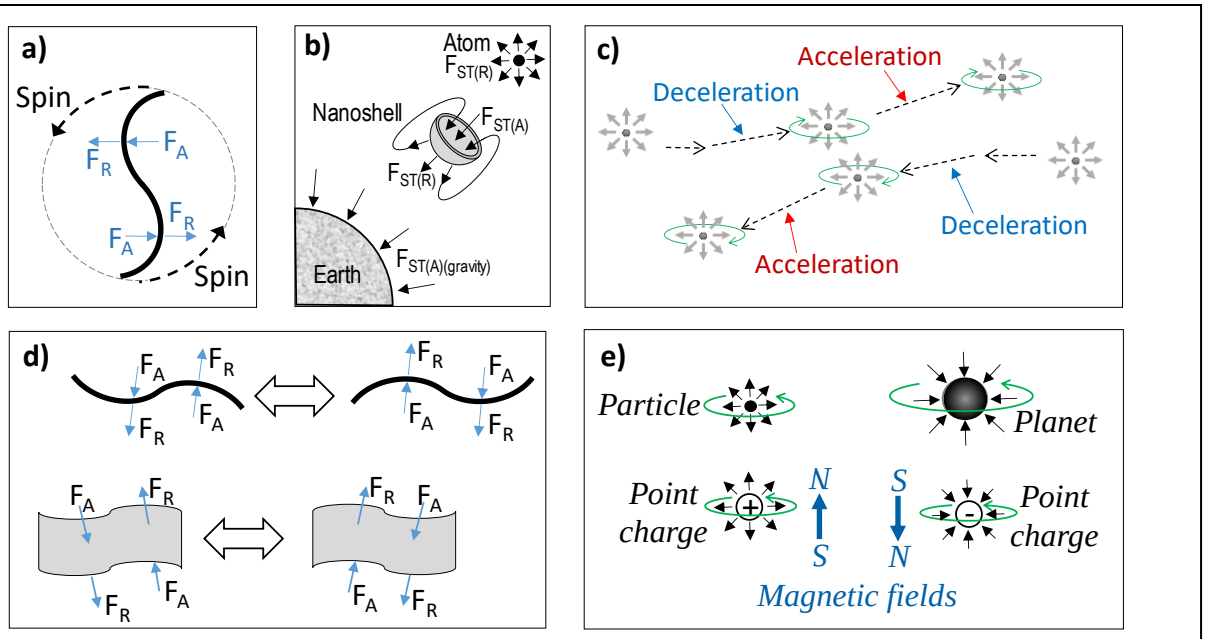

Fig. 2. Schematics of F_{ST} interaction, migration, rotation, vibration and oscillation. In between the S-shaped string's convex and concave surfaces (**a),** Earth, nanoshell, and atom (**b**), migrating particles **(c)**, thermally vibrating and oscillating string's and membrane's curving surfaces **(d)**, and spinning particle, planet, and point-charges **(d).**

mechanics and dynamics in Newton's Laws of Motion and Wheeler's Geometrodynamic Gravitation[14,15].

Countering bigger planets' greater F_A that pulls the planets closer (**Supplementary Fig. S2**), smaller particles' surface greater $F_{ST(R)}$ repel the particles farther apart each other (**Fig. 2c**). This supports smaller particles greater incapability of collision (matching the Ideal Gas Law, and a particle collider's need of high energy-input), faster Brownian motion (i.e. nonstop acceleration, deceleration, and rotation), lower boiling and freezing points, and greater chaosity (or Boltzmann entropy i.e. thermodynamics).

So, smaller particles in faster rotation, acceleration and deceleration should interact more using their greater F_{ST}, emitting waves in stronger diffractions upon passing through two thinner and closer slits[16] (i.e. four matter-vacuum interfaces). This supports the E_{ST} in

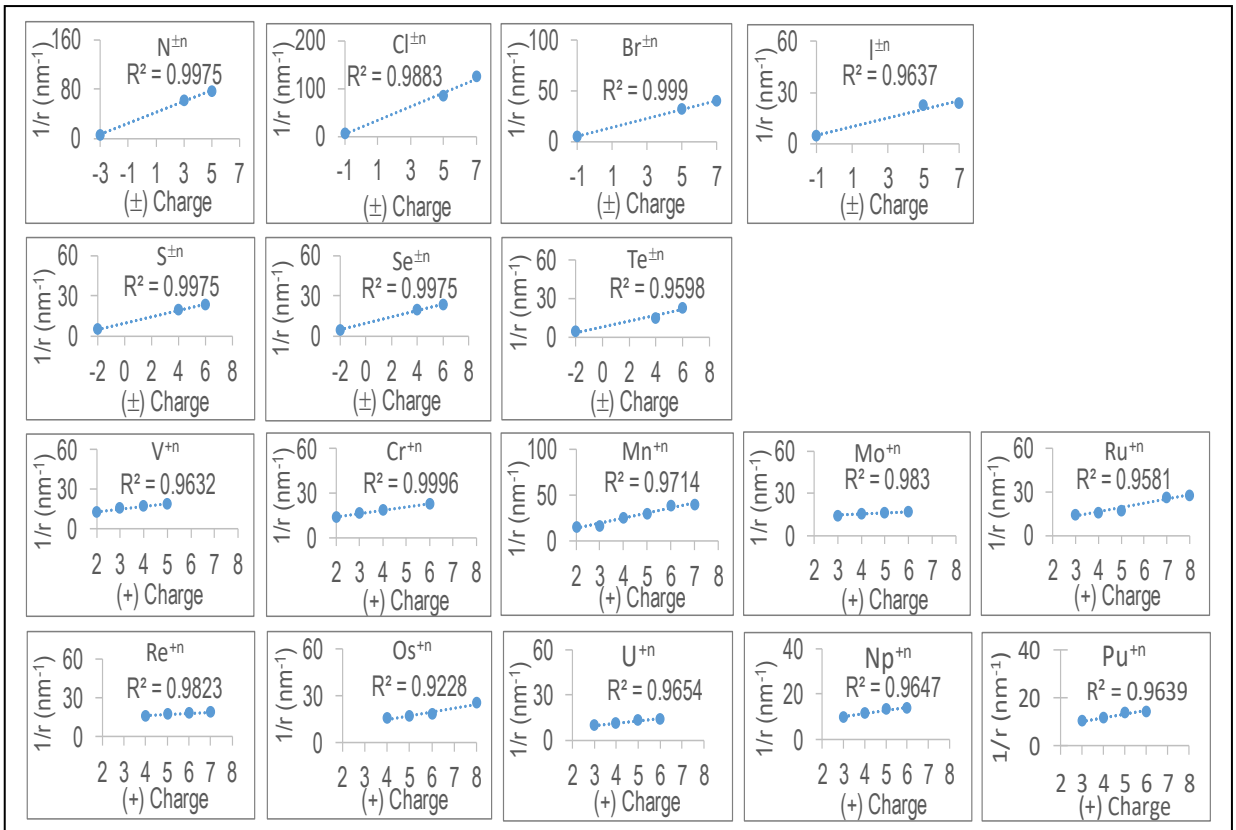

Fig. 3. The apparent coupling of F_{EM} and F_{ST} in monoatomic cations' and anions' (1/r) values.

governing the QM's wave–particle dualism[17] and quantum entanglement[18].

Further, thinner and longer wires and membranes can use their edge's and curving surface's higher $E_{ST(Levity)}$ to energize nearby smaller particles to migrate in a higher speed (or momentum) over a longer mean free path on the edge and surface. This supports the F_{ST} in motor proteins' quicker migration on thinner nanowires[19] and rapid charge transfer on thousands of topological insulators[20].

Logically, the DNA- and α-helices edges' E_{ST} should energize nearby molecules and ions to spiral rapidly along the edge to activate countless chemical changes. This helps expand the chemical bonding theory[3] to considering the E_{ST} and E_{ST}-spun Φ_{ST}. Thus, on thinner strings and membranes in higher thermal vibration or oscillation (**Fig. 2d**), the greater $E_{ST(Surface)}$ should support the Tribo-energy Nanogenerators[21], String Theory[22], and M-Theory[23].

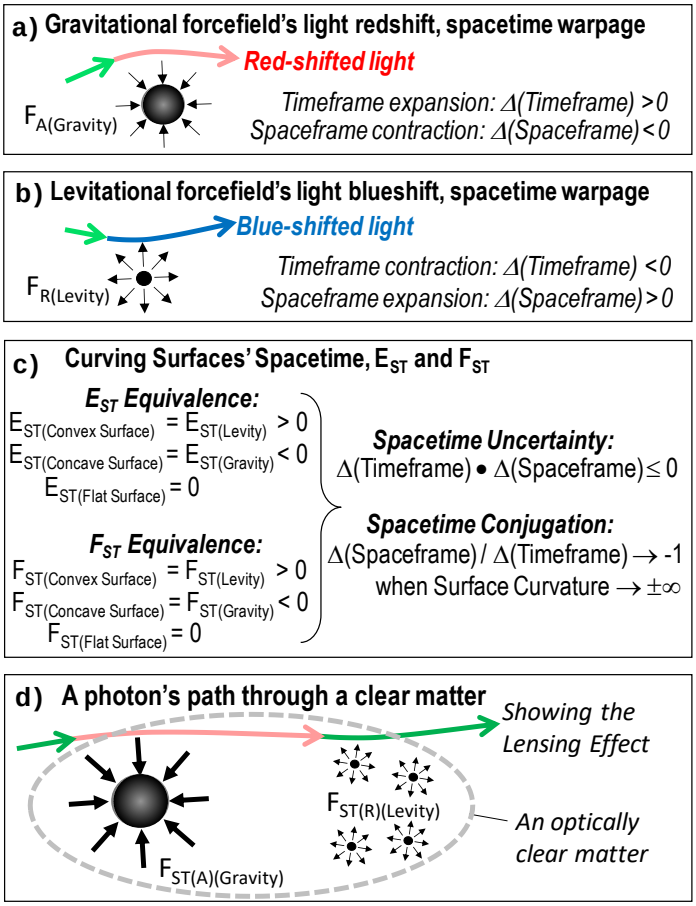

Fig. 4. The Warping Spacetimes' Energy and Forcefield for Gravity (a), Levity (b), their Uncertainty, Conjugation, and Equivalences (c), and for a Clear Matter (d).

Thus, a spinning particle's rotating F_{ST} can couple with an oppositely spinning particle's and with a spinning planet's, as spinning point-charges do (**Fig. 2e**). This can help expand Maxwell Equations[24], e.g. $\oint \vec{E}_{ST} \cdot d\vec{A}_{ST} \approx -d\Phi_{ST}/dt$, where the $\vec{A}_{ST} = \vec{E}_{ST}$ flux area, and Φ_{ST} = F_{ST}-rotated magnetics flux (stronger on a neutron star[25] in spin than that on the Earth). This supports (see the **Supplementary Table S2**) ions' charge-based (1/r) values (**Fig. 3**).

Countering the gravity-induced light redshift[26,27] (**Fig. 4a**), the semiconducting NPs' optical bandgap blueshift (**Fig. 1, a-d**) does quantify their gravity-counterbalancing property i.e. **levity**, namely (**Fig. 4b**). The greater levity on a smaller particle's surface can help quantize and generalize Einstein's

spacetime in all abovementioned cases, and more below.

First, the levity-contracted timeframe and levity-expanded spaceframe (**Fig. 4b**) support the small concave, convex and flat surfaces' spacetimes; Spacetime Conjugation i.e. Δ*(Spaceframe)*/Δ*(Timeframe)* ≈ -1 when (surface-curvature) $\rightarrow \pm\infty$; and Spacetime Uncertainty or Δ*(Spaceframe)*·Δ*(Timeframe)* $\leq$ *0* (**Fig. 4c**). This can help geometrize particles' surface-warped spacetimes in Heisenberg's Uncertainty[28]. As the vacuum- and matter-spacetimes warp oppositely at their interface, the $E_{ST(levity)} = E_{ST(convex\ matter\ surface)} = E_{ST(concave\ vacuum\ surface)}$, and $E_{ST(gravity)} = E_{ST(concave\ matter\ surface)} = E_{ST(convex\ vacuum)}$, all useful in the surface geometrochemistry.

Second, a photon shouldn't change its wavelength after traveling through a group of matters along a path with the gravity-redshift(s) offsetting the levity-blueshift(s), as if through a lens-like clear matter looking "invisible" (or "dark") against the dark cosmic background (**Fig. 4d**). Thus, the clear (or "dark") matter's spacetime-offsetting degree tells its clearness (or "darkness"), and its geometry does the Lensing Effect[29], thus-enriching the geometro-cosmochemistry.

Third, the Earth's gravity can couple constructively in a pinhole with the concave surface's gravity-equivalent $F_{ST(A)}$ but destructively on a pin tip with the convex surface's levity-equivalent $F_{ST(R)}$. This can help predict and compare quantitatively all smaller pores', tips', and edges' higher geometrochemical reactivity (i.e. energy).

In addition, on a matter's curving surface the $F_{ST(surface)} = E_{ST}/r = \pm(hc/r^2)$, like the $F_{(Coulomb)}$ (i.e. kq_1q_2/r^2) and $F_{(Gravity)}$ (i.e. $G{\cdot}m_1{\cdot}m_2/r^2$), which supports the forcefields- and curving spacetimes-rotated magnetics. More generally, Einstein's $E_{(Gravity)}$-offseter[30] i.e. Dark Energy $E_{(Dark)} \equiv E_{ST(Levity)} = hc/r \neq$ constant, which exists everywhere including the geometrochemistry and geometrochemical biology.

In summary, the SCEE-induced E_{ST} and levity support both well-established laws and spacetime-generalized sciences (**Fig. 5**). The warping spacetimes migration-, rotation-, vibration- and interaction-based mechanics, dynamics, kinetics, energetics, and magnetics will inspire new experimental verifications and technological innovations.

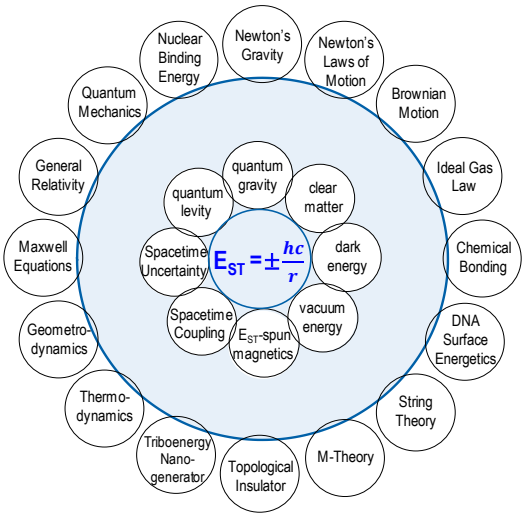

Fig. 5. The E_{ST}'s eight derivations and 16 links.

EFERENCES:

[1] Tian, Z. Nanoparticles' and Atoms' Geometry-Wave Potential Quantified and Unified Properties. *ChemRxiv*. Preprint (Sept. 5, 2019). https://doi.org/10.26434/chemrxiv.9759551.v1.

[2] Tian, Z. Geometry-Wave Potential Quantified and Unified Properties in General Chemistry. *ChemRxiv*. Preprint (Sept. 5, 2019). https://doi.org/10.26434/chemrxiv.9759581.v1.

[3] Pauling, L. *The Nature of Chemical Bond* (Cornell U. Press, 1960). ISBN-10: 0801403332.

[4] Rossetti, R.; Nakahara, S. and Brus, L. E. Quantum size effects in the redox potentials, resonance Raman spectra, and electronic spectra of CdS crystallites in aqueous solution, *J. Chem. Phys*. **79**, 1086–1088 (1983). doi.org/10.1063/1.445834.

[5] Murray, C. B.; Norris, D. J. and Bawendi, M. G. Synthesis and characterization of nearly monodisperse CdE (E = Sulfur, Selenium, Tellurium) semiconductor nanocrystallites, *J. Am. Chem. Soc*. **115**, 8706–8715 (1993). doi.org/10.1021/ja00072a025.

[6] Vossmeyer, T.; Katsikas, L.; Giersig, M.; Popovic, I. G.; Diesner, K.; Chemseddine, A.; Eychmueller, A. and Weller, H. CdS Nanoclusters: Synthesis, Characterization, Size Dependent Oscillator Strength, Temperature Shift of the Excitonic Transition Energy, and Reversible Absorbance Shift. *J. Phys. Chem.* **98**, 7665–7673 **(**1994**)**. doi.org/10.1021/j100082a044.

[7] Yu, W. W.; Qu, L.; Guo, W. and Peng, X. Experimental determination of the extinction coefficient of CdTe, CdSe, and CdS nanocrystals. *Chem. Mater*. **15** (14), 2854–2860 (2003). doi.org/10.1021/cm034081k.

[8] Moreels, I.; Lambert, K.; De Muynck, D.; Vanhaecke, F.; Poelman, D.; Martins, J. C.; Allan, G. and Hens, Z. Composition and size-dependent extinction coefficient of colloidal PbSe quantum dots, *Chem. Mater*. **19**, 6101–6106 (2007). doi.org/10.1021/cm071410q.

[9] *Gold Nanoparticles: Properties and Applications*, Sigma-Aldrich, (www.sigmaaldrich.com/technical-documents/articles/materials-science/nanomaterials/gold-nanoparticles.html).

[10] Basdevant, J.-L.; Rich, J. and Spiro, M. *Fundamentals in nuclear physics* (Springer, 2005). ISBN-10: 1441918493.

[11] Fewell, M. P. The atomic nuclide with the highest mean binding energy, *Am. J. Phys*. **63** (7), 653-658 (1995). doi.org/10.1119/1.17828.

[12] Einstein, A. Does the inertia of a body depend upon its energy-content? *Annalen der Physik*, **18**, 639–643 (1905). http://www.astro.puc.cl/~rparra/tools/PAPERS/e_mc2.pdf.

[13] de Broglie, L. The Reinterpretation of Wave Mechanics. *Foundations of Physics* **1**, 1 (1970). https://link.springer.com/article/10.1007/BF00708650.

[14] Wheeler, J. A. *Geometrodynamics* (Academic Press, New York, 1963). LCCN 62013645.

[15] Misner, C. W.; Thorn, K. S. and Wheeler, J. A. *Gravitation* (W. H. Freeman, 1973). ISBN 0-7167-0334-3.

[16] Schrödinger, E. Probability relations between separated systems. *Math. Proceed. Cambridge Phil. Soc.* **32**, 446–452 (1936). DOI: https://doi.org/10.1017/S0305004100019137.

[17] Einstein, A.; Podolsky, B. and Rosen, N. Can quantum-mechanical description of physical reality be considered complete? *Phys. Rev.* **47**, 777–780 (1935). doi:10.1103/PhysRev.47.777.

[18] Greiner, W. *Quantum Mechanics: An Intro* (Springer, 2001). ISBN 978-3-540-67458-0.

[19] Berg, J. M.; Tymoczko, J. L. and Stryer, L. *Biochemistry* (W. H. Freeman, New York, 2002). ISBN-10: 0-7167-3051-0.

[20] Gibney, E. Thousands of exotic 'topological' materials discovered through sweeping search. *Nature*, **560**, 151-152 (2018). doi: 10.1038/d41586-018-05913-4.

[21] Wu, C.; Wang, A. C.; Ding, W.; Guo, H. and Wang, Z. L. Triboelectric Nanogenerator: A Foundation of the Energy for the New Era, *Adv. Energy Mat*, **9**, 1 (2018). doi.org/10.1002/aenm.201802906.

[22] Green, M.; Schwarz, J. and Witten, E. *Superstring theory. Vol. 1: Introduction*. (Cambridge University Press, 2012). ISBN 978-1107029118.

[23] Witten, E. String theory dynamics in various dimensions. *Nuclear Phys.* B. **443**, 85–126 (1995). doi:10.1016/0550-3213(95)00158-O.

[24] Fitzpatrick, R. *Maxwell's Equations and the Principles of Electromagnetism* (Infinity Science Press, Hingham, MA 2008). https://www.fisica.net/ebooks/eletricidade/FITZPATRICK%20-%20Maxwell's%20equations%20and%20the%20principle%20of%20electromagnetism.pdf.

[25] Reisenegger, A. Origin and evolution of neutron star magnetic fields, https://arxiv.org/abs/astro-ph/0307133.

[26] Forbes, E. G. A history of the solar red shift problem. *Annals of Science*, **17**(3), 129-164 (1961). doi.org/10.1080/00033796100202601.

[27] Einstein, A. Die Grundlage der allgemeinen Relativitätstheorie Annalen der Physik, 49 (1916). *Reprinted in English translation in The Principle of Relativity*. (Dover Publications Inc, New York, 1952). http://www.synergiecomunicazione.it/eventime/Abstract.pdf.

[28] Heisenberg, W. Über den anschaulichen Inhalt der quantentheoretischen Kinematik und Mechanik, *Zeitschrift für Physik*. **43**, 172–198 (1927). doi.org/10.30965/9783846757123_004.

[29] Refregier, A. Weak gravitational lensing by large-scale structure. *Annual Rev. Astronomy Astrophysics*. **41** (1), 645–668 (2003). https://arxiv.org/abs/astro-ph/0307212.

[30] Einstein, A. Kosmologische Betrachtungen zur allgemeinen Relativitätstheorie, (Cosmological Considerations in the General Theory of Relativity) *Koniglich Preußische Akademie der Wissenschaften, Sitzungsberichte* (Berlin): 142–152 (1917). .http://echo.mpiwg-berlin.mpg.de/ECHOdocuView?url=/permanent/echo/einstein/sitzungsberichte/S250UZ0K/index.meta&pn=1.

EXTENDED DATA

I. Supplementary Information.

II. Supplementary Tables S1 & S2.

III. Supplementary Figures S1&S2.

IV. References.

Title: **Surface curvature-quantized energy and forcefield in geometrochemical physics**

Z. R. Tian, Chemistry/Biochemistry, and Materials Science/Engineering, University of Arkansas, Fayetteville, AR 72701, USA, (Email) rtian@uark.edu.

I. Supplementary Information:

If six nucleons were hypothetically close-packed, the octahedral void's center-spherical radius $r_{(void)} \approx 0.414 \cdot r_{(nucleon)}$[1], and $E_{ST(void)} \approx -(3.1/0.414) = -7.49$ (GeV), although the six nucleons' Nuclear Binding Energy[2,3] (E_{NB}) ≤ 0.060 (GeV), i.e. $E_{NB} << |E_{ST(void)}|$. The similar from hypothetically close-packing four nucleons into a tetrahedron. Equivalently, the E_{ST}-energized nucleons cannot be close-packed, not to mention the close-packing of the much smaller quarks. This trend supports logically the Spacetime Conjugation, Spacetime Uncertainty and Heisenberg's Uncertainty for nucleons in a nucleus, and for "massless" elementary particles in a nucleon.

II. Supplementary Table S1a[4,5]:

Spherical (0D) NPs' (1/r), optical bandgap (E_{BG}) data

(a) CdTe NPs	
E_{BG} (eV)	1/r (nm^{-1})
2.58	0.83
2.48	0.70
2.28	0.60
2.13	0.53
2.04	0.50
1.97	0.47
1.93	0.40
1.88	0.40
1.82	0.37
1.74	0.27
1.68	0.23
1.64	0.21
1.62	0.18

(b). CdSe NPs	
E_{BG} (eV)	1/r (nm^{-1})
3.00	1.63
2.57	0.93
2.45	0.87
2.25	0.58
2.21	0.53
2.09	0.46
2.05	0.41
1.98	0.39
1.84	0.24
1.81	0.18

(c) CdS NPs	
E_{BG} (eV)	1/r (nm^{-1})
4.78	3.1
4.22	2.8
3.89	2.5
3.72	2.2
3.32	1.0
3.05	0.70
2.68	0.43

(d). PbSe NPs	
E_{BG} (eV)	1/r (nm^{-1})
0.833	0.39
0.967	0.47
1.077	0.53
1.243	0.63
1.656	0.87

II. Supplementary Table S1b[4,5]:

Spherical (0D) NPs' (1/r) and melting point (T_m) data

(e). Au NPs	
1/r (nm^{-1})	T_m (^oK)
0.750	853.16
0.600	973.16
0.500	1053.16
0.429	1103.16
0.375	1143.16
0.333	1163.16
0.300	1183.16
0.273	1193.16
0.250	1213.16
0.231	1223.16
0.214	1228.16
0.200	1233.16
0.188	1241.16
0.176	1245.16
0.167	1248.16
0.158	1251.16
0.150	1254.16

II. Supplementary Table S1c[4,5]:

Main-groups atoms' (1/r) and EN data

Atom	1/r (nm^{-1})	**EN**
Li	6.87	0.98
Be	8.93	1.57
B	11.5	2.04
C	14.9	2.55
N	17.9	3.04
O	20.8	3.44
F	23.8	3.98
Na	5.27	0.93
Mg	6.90	1.31
Al	8.47	1.61
Si	9.03	1.90
P	10.2	2.19
S	11.4	2.58
Cl	12.7	3.16
K	4.13	0.82
Ca	5.17	1.00
Ga	7.37	1.81
Ge	8.00	2.01
As	8.77	2.18
Se	9.73	2.55
Br	10.6	2.96

Atom	1/r (nm^{-1})	**EN**
Rb	3.77	0.82
Sr	4.57	0.95
In	6.43	1.78
Sn	6.90	1.96
Sb	7.53	2.05
Te	8.13	2.10
I	9.73	2.66
Cs	3.37	0.79
Ba	3.97	0.89
Tl	6.43	1.62
Pb	6.50	1.87
Bi	7.00	2.02
Po	7.40	2.00
At	7.87	2.20

II. Supplementary Table S2[4,5] of Multivalent Monoatomic Ions' Radii and (1/r) Values

Ion	Charge	r (nm)	1/r (nm^{-1})	Ion	Charge	r (nm)	1/r (nm^{-1})	Ion	Charge	r (nm)	1/r (nm^{-1})
Cl^{-}	-1	0.181	5.52	V^{+2}	2	0.079	12.7	Re^{+4}	4	0.063	15.9
Cl^{+5}	5	0.012	83.3	V^{+3}	3	0.064	15.6	Re^{+5}	5	0.058	17.2
Cl^{+7}	7	0.008	125	V^{+4}	4	0.058	17.2	Re^{+6}	6	0.055	18.2
				V^{+5}	5	0.054	18.5	Re^{+7}	7	0.053	18.9
Br^{-}	-1	0.196	5.10								
Br^{+5}	5	0.031	32.3	Cr^{+2}	2	0.073	13.7	Os^{+4}	4	0.063	15.9
Br^{+7}	7	0.025	40.0	Cr^{+3}	3	0.062	16.1	Os^{+5}	5	0.058	17.2
				Cr^{+4}	4	0.055	18.2	Os^{+6}	6	0.055	18.2
I^{-}	-1	0.220	4.55	Cr^{+6}	6	0.044	22.7	Os^{+8}	8	0.039	25.6
I^{+5}	5	0.044	22.7								
I^{+7}	7	0.042	23.8	Mn^{+2}	2	0.066	15.2	U^{+3}	3	0.103	9.71
				Mn^{+3}	3	0.058	17.2	U^{+4}	4	0.089	11.2
S^{-2}	-2	0.184	5.43	Mn^{+4}	4	0.039	25.6	U^{+5}	5	0.076	13.1
S^{+4}	4	0.037	27.0	Mn^{+5}	5	0.033	30.3	U^{+6}	6	0.073	13.7
S^{+6}	6	0.029	34.5	Mn^{+6}	6	0.026	38.5				
				Mn^{+7}	7	0.025	40.0	Np^{+3}	3	0.101	9.90
Se^{-2}	-2	0.198	5.05					Np^{+4}	4	0.087	11.5
Se^{+4}	4	0.050	20.0	Mo^{+3}	3	0.069	14.5	Np^{+5}	5	0.075	13.3
Se^{+6}	6	0.042	23.8	Mo^{+4}	4	0.065	15.4	Np^{+6}	6	0.072	13.9
				Mo^{+5}	5	0.061	16.4				
Te^{-2}	-2	0.221	4.52	Mo^{+6}	6	0.059	16.9	Pu^{+3}	3	0.100	10.0
Te^{+4}	4	0.066	15.2					Pu^{+4}	4	0.086	11.6
Te^{+6}	6	0.043	23.3	Ru^{+3}	3	0.068	14.7	Pu^{+5}	5	0.074	13.5
				Ru^{+4}	4	0.062	16.1	Pu^{+6}	6	0.071	14.1
N^{-3}	-3	0.171	5.85	Ru^{+5}	5	0.057	17.5				
N^{+3}	3	0.016	62.5	Ru^{+7}	7	0.038	26.3				
N^{+5}	5	0.013	76.9	Ru^{+8}	8	0.036	27.8				

III. Supplementary Figures:

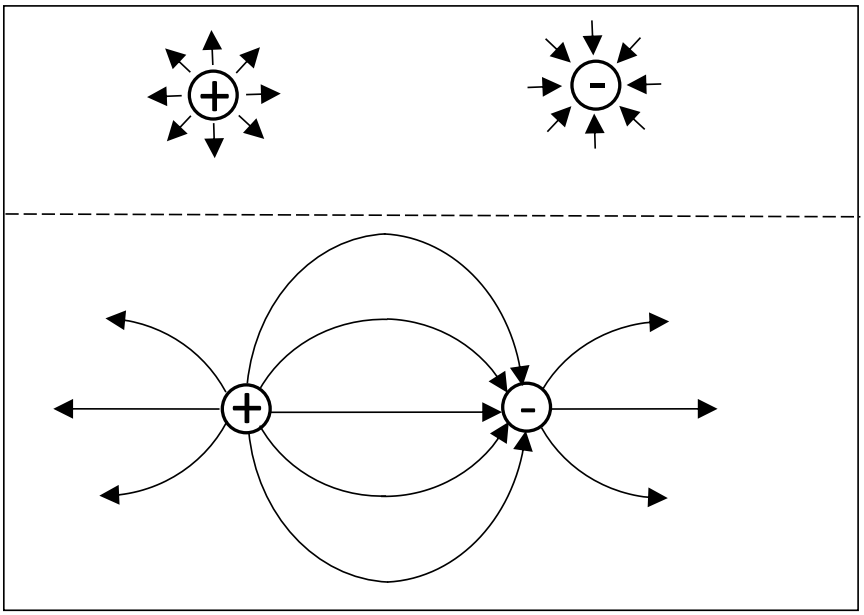

Fig. S1. Positive point-charge's outward forcefield, negative point-charge's inward forcefield, and the two forcefields' coupling.

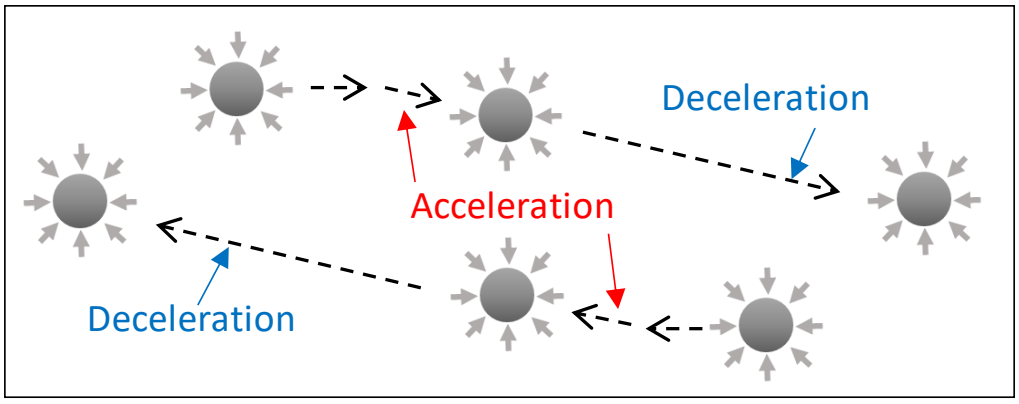

Fig. S2. Gravitational forcefields interaction between passing-by planets

IV. References:

[1] Wells, A. F. *Structural Inorganic Chemistry* (Oxford, 2012). ISBN-10: 0198553706.

[2] Basdevant, J.-L.; Rich, J. and Spiro, M. *Fundamentals in nuclear physics* (Springer, 2005). ISBN 0-387-01672-4.

[3] Fewell, M. P. The atomic nuclide with the highest mean binding energy, *Am. J. Phys*. **63** (7), 653-658 (1995). doi.org/10.1119/1.17828.

[4] Tian, Z. Nanoparticles' and Atoms' Geometry-Wave Potential Unified Properties. *ChemRxiv*. Preprint (Sept. 5, 2019). https://doi.org/10.26434/chemrxiv.9759551.v1.

[5] Tian, Z. Geometry-Wave Potential Quantified and Unified Properties in General Chemistry. *ChemRxiv*. Preprint (Sept. 5, 2019). https://doi.org/10.26434/chemrxiv.9759581.v1.